DOMAIN DECOMPOSITION METHODS COUPLED WITH PARAREAL FOR THE TRANSIENT HEAT EQUATION IN 1 AND 2 SPATIAL DIMENSIONS

LADISLAV FOLTYN, Ostrava, DALIBOR LUKÁŠ, Ostrava, IVO PETEREK, Ostrava

Abstract. We present a parallel solution algorithm for the transient heat equation in one and two spatial dimensions. The problem is discretized in space by the lowest-order conforming finite element method. Further, a one-step time integration scheme is used for the numerical solution of the arising system of ordinary differential equations. For the latter the parareal method decomposing the time interval into subintervals is employed. It leads to parallel solution of smaller time-dependent problems. At each time slice a pseudo-stationary elliptic heat equation is solved by means of a domain decomposition method (DDM). In the 2d case it is replaced by a nonoverlapping Schur complement method, while in the 1d case an overlapping Schwarz DDM is employed. We document computational efficiency as well as theoretical convergence rates of FEM semi-discretization schemes on numerical examples.

Keywords: domain decomposition methods, parareal, finite element method, heat equation

MSC 2010: 65N55, 65N30, 65F08

1. INTRODUCTION

Domain decomposition methods (DDM) are well-established techniques of parallel numerical solution to boundary value problems for elliptic partial differential equations (PDE). The problem is typically discretized by means of the finite element method leading to a system of linear equations. The discretization usually aligns with a decomposition of the computational domain into either overlapping [20] or nonoverlaping [22] subdomains. This results in a number of PDE subproblems that can be solved in parallel. The concurrent subproblems are coupled via a global coarse

problem of a much smaller size than the original system. In case of nonoverlapping DDM there are methods of balancing domain decomposition [16], finite element tearing and interconnecting [5], or Schur complement methods [1] to name a few. All these methods combine direct methods for the subdomain and coarse problems to build a preconditioner for an iterative method applied to the original large system. The condition number of such a preconditioned system is only poly-logarithmic in terms of H/h, where H is a typical subdomain diameter and h denotes the FEM discretization step. The methods enjoy strong parallel scalability meaning that both the computational time and memory consumption is inversely proportional to the number of computational cores.

The situation becomes more difficult in case of time-evolving PDEs. Due to the fact that the solution to an evolution problem at a time instance depends only on the previous time instances it was believed that it would not be possible to break this sequential nature and develop a parallel solution algorithm. In 2001 Lions, Maday, and Turinici published a breakthrough paper [14] in this regard. They introduced the parareal method for parallel-in-time solution of first-order differential equations. The method decomposes the time interval into subintervals and combines concurrent local fine integrators with a global coarse integrator in the sense of a predictor-corrector technique. The convergence of the method was proven in [11, 12] to be super-linear on bounded and linear on unbounded time intervals. In [12] connections to the multiple shooting method as well as multigrid were shown. In [4] the parareal method is presented as a two-grid Newton method. The authors further deliver a parallel speedup analysis and a feasibility study towards fluid simulations and structural analysis, the latter of which proves some instability issues. Stability for hyperbolic systems was later recovered in [2]. Many engineering applications of the parareal method were done, cf. [17, 19].

Besides the parareal method discretizing the PDE in the time direction waveform relaxation methods have been developed. They generalize DDM such that concurrent time-dependent local problems are solved on spatial subdomains throughout the whole time interval. Nonoverlapping Neumann-Neumann and Dirichlet-Neumann Schwarz methods applied to 1-dimensional heat equation with some preliminary results in 2 dimensions is presented in [9]. The overlapping Schwarz applied to 1-dimensional wave equation is presented in [7, 8].

Finally, there has been done a lot of interesting work in the direction of parallel-in-time multigrid methods. In [18, 10] a parallel space-time multigrid method is proposed and analyzed for the discontinuous-in-time and continuous-in-space Galerkin method for parabolic problems. Numerical results proving parallel scalability up to billions of degrees of freedom are given for 2-dimensional heat as well as Navier-Stokes equations with geometry evolving in time. Another approach combining a

finite-difference multigrid method in space with the parareal method is presented in [3].

In this paper we propose a combination of the parareal and DDM for the heat equation. In Section 2 we recall the weak formulation of the heat equation, we discretize it by the finite element method in space and recall the convergence theory of the FEM approximations towards the space-time weak solution. In Section 3 we recall the parareal method, a 2-dimensional nonoverlapping Schur complement method and a 1-dimensional overlapping Schwarz DDM. In Section 4 we present numerical results confirming the FEM convergence theory, the efficiency of the parareal method and its combination with two DDMs, a one of which is novel.

2. FINITE ELEMENT SEMI-DISCRETIZATION OF THE TRANSIENT HEAT EQUATION

We consider the following initial boundary value problem for the heat equation:

$$
(2.1) \quad
\begin{cases}
c(x)\frac{\partial u}{\partial t}(x,t) - \operatorname{div}\left(k(x)\nabla u(x,t)\right) &=& f(x,t), & x \in \Omega,\ t \in I, \\
u(x,t) &=& 0, & x \in \Gamma_{\mathrm{D}},\ t \in I, \\
k(x)\frac{\partial u}{\partial n}(x,t) &=& g(x,t), & x \in \Gamma_{\mathrm{N}},\ t \in I, \\
u(x,0) &=& u_0(x), & x \in \Omega,
\end{cases}
$$

where we search for the temperature distribution $u(x,t)$ in the spatial domain $\Omega \subset \mathbb{R}^d$, $d = 1, 2$, and int the time interval $I := (0, T)$. The functions $c(x)$ and $k(x)$ are the spatial distributions of the heat capacity and the heat conductivity, respectively, and $f(x,t)$ denotes the volume heat sources. The boundary $\Gamma := \partial\Omega$ is decomposed into two nonoverlapping components — the Dirichlet part Γ_{D}, on which we prescribe the zero temperature, and the Neumann part Γ_{N}, on which a numerical flux g is prescribed. By n we denote the unit normal vector outward to Ω, and u_0 is the spatial distribution of the initial temperature.

Let $V := H^1_{0,\Gamma_{\mathrm{D}}}(\Omega)$. The weak formulation of (2.1) reads to find $u \in L^2(I, H^1(\Omega))$ such that $\frac{\partial u}{\partial t} \in L^2(I, V^*)$, $u(x,0) = u_0(x)$ a.e. in Ω, and for almost all $t \in I$:

$$
(2.2) \quad \int_\Omega c(x)\,\frac{\partial u}{\partial t}(x,t)\,v(x)\,dx + \int_\Omega k(x)\,\nabla_x u(x,t)\cdot\nabla v(x)\,dx
$$

$$
= \int_\Omega f(x,t)\,v(x)\,dx + \int_{\Gamma_{\mathrm{N}}} g(x,t)\,v(x)\,ds(x) \quad \forall v(x) \in V.
$$

The following theorem is a direct consequence of [23, Th.23.A].

Theorem 2.1. *Let $I := (0, T)$, $T > 0$, and let $\Omega \subset \mathbb{R}^d$, $d = 1, 2$, be a bounded simply-connected domain with Lipschitz boundary, which consists of two nonoverlapping Lebesque measurable components Γ_{D} and Γ_{N} with $\operatorname{meas}\Gamma_{\mathrm{D}} > 0$. Assume further that $u_0 \in L^2(\Omega)$, $f \in L^2(\Omega \times I)$, $g \in L^2(\Gamma_{\mathrm{N}} \times I)$, and $c, k \in L^\infty(\Omega)$ be such*

that $c(x) \geq c_0 > 0$ and $k(x) \geq k_0 > 0$ a.e. in Ω. Then there exists a unique solution u to (2.2), which continuously depends on the data, i.e., there exists $C > 0$ such that

$$\|u\|_{L^2(I;V)} + \|u'\|_{L^2(I;V^*)} \leq C \left(\|u_0\|_{L^2(\Omega)} + \|f\|_{L^2(\Omega \times I)} + \|g\|_{L^2(\Gamma_{\mathrm{N}} \times I)} \right).$$

We recall that the norm in the Bochner-Lebesque space $L^2(I, B)$, where B is a Banach space, is defined as follows:

$$\|u\|_{L^2(I;B)} := \left(\int_I \|u(t)\|_B^2 \, dt \right)^{1/2}.$$

We introduce a shape-regular and quasi-uniform finite element triangulation of Ω and the conforming finite element subspace $V^h := \mathrm{span}(\phi_1(x), \dots, \phi_n(x)) \subset V$, where $\phi_i(x)$ is the element-wise linear nodal FEM basis function. The Galerkin approximation of (2.2) results in the following Cauchy problem for linear system of the first-order ordinary differential equations:

(2.3)
$$\begin{cases} \mathbf{M} \cdot \mathbf{u}'(t) + \mathbf{K} \cdot \mathbf{u}(t) & = \quad \mathbf{b}(t) \qquad \forall t \in I, \\ \mathbf{u}(0) & = \quad \mathbf{u}_0, \end{cases}$$

where for $i, j = 1, \dots, n$, $(\mathbf{M})_{ij} := \int_\Omega c \phi_j \phi_i$, $(\mathbf{K})_{ij} := \int_\Omega k \nabla \phi_j \nabla \phi_i$, $(\mathbf{b}(t))_i := \int_\Omega f(t) \phi_i + \int_{\Gamma_{\mathrm{N}}} g(t) \phi_i$, $u_0^h(x) := \sum_{j=1}^n (\mathbf{u}_0)_j \phi_j(x)$ is an approximation of $u_0(x)$. The approximate solution reads as follows:

(2.4)
$$u^h(x, t) := \sum_{j=1}^n (\mathbf{u}(t))_j \phi_j(x).$$

Note that the unique solvability of problem (2.3) follows from the fact that both $\mathbf{M}$ and $\mathbf{K}$ are symmetric positive definite.

From [21, Th.1.2,1.3] we have the following convergence result.

Theorem 2.2. *Let the assumptions of Theorem 2.1 hold true. Further, let $\Gamma_{\mathrm{D}} := \Gamma$, i.e., $\Gamma_{\mathrm{N}} = \emptyset$, u^h be the solution to (2.3), (2.4), and u be the solution to (2.2). Assume $u_0^h = 0$ on Γ. Then there exists $C > 0$ independent of h such that for $r \in [1, 2]$ and $t \geq 0$:*

$$\|u^h(x, t) - u(x, t)\|_{L^2(\Omega)} \leq \|u_0^h(x) - u_0(x)\|_{L^2(\Omega)} +$$
$$C \, h^r \left(\|u_0(x)\|_{H^r(\Omega)} + \int_0^t \left\| \frac{\partial u}{\partial s}(x, s) \right\|_{H^r(\Omega)} ds \right)$$

and

$$\|\nabla\, u^h(x,t) - \nabla\, u(x,t)\|_{L^2(\Omega)} \le \|\nabla\, u_0^h(x) - \nabla\, u_0(x)\|_{L^2(\Omega)} +$$

$$+ C\, h^{r-1} \left\{ \|u_0(x)\|_{H^r(\Omega)} + \|u(x,t)\|_{H^r(\Omega)} + \left(\int_0^t \left\| \frac{\partial u}{\partial s}(x,s) \right\|_{H^{r-1}(\Omega)}^2 ds \right)^{1/2} \right\}.$$

Finally, we employ time-stepping schemes. We decompose I into m time intervals (t_{k-1}, t_k), where $t_k := k\,\delta t$, $k = 0, 1, \dots, m$, and $\delta t := T/m$. In the backward Euler time-stepping method the time derivative is approximated by the backward difference

$$\mathbf{u}'(t_k) \approx \frac{1}{\delta t}\left(\mathbf{u}_k - \mathbf{u}_{k-1}\right),$$

where $\mathbf{u}_k := \mathbf{u}(t_k)$. Hence, we sequentially solve the following linear systems:

$$(2.5) \qquad (\mathbf{M} + \delta t\,\mathbf{K}) \cdot \mathbf{u}_k = \delta t\,\mathbf{b}_k + \mathbf{M} \cdot \mathbf{u}_{k-1}, \; k \ge 1,$$

where $\mathbf{b}_k := \mathbf{b}(t_k)$. The approximate solution reads

$$(2.6) \qquad u_k^h(x) := \sum_{j=1}^{n} (\mathbf{u}_k)_j\, \phi_j(x).$$

From [21, Th.1.5] we have the following convergence result.

Theorem 2.3. *Let the assumptions of Theorem 2.2 hold true. Further, let u_k^h, $k \ge 0$, be the solution to (2.5), (2.6), and let there exist $K > 0$ independent of h such that for all $r \in [1,2]$:*

$$\|u_0^h(x) - u_0(x)\|_{L^2(\Omega)} \le K\, h^r \|u_0(x)\|_{H^r(\Omega)}$$

and $u_0(x) = 0$ on Γ. Then, there exists $C > 0$ such that for $k \ge 0$ and $r \in [1,2]$ it holds that

$$\|u_k^h(x) - u(x,t_k)\|_{L^2(\Omega)} \le$$

$$C\, h^r \left(\|u_0(x)\|_{H^r(\Omega)} + \int_0^{t_k} \left\| \frac{\partial u}{\partial s}(x,s) \right\|_{H^r(\Omega)} ds \right) + \delta t \int_0^{t_k} \left\| \frac{\partial^2 u}{\partial s^2}(x,s) \right\|_{L^2(\Omega)} ds.$$

A higher convergence-in-time rate can be achieved by employing the Crank-Nicolson scheme. We arrive at the following sequence of linear systems:

$$(2.7) \qquad \left(\mathbf{M} + \frac{1}{2}\delta t\,\mathbf{K}\right) \cdot \mathbf{u}_k = \delta t\,\mathbf{b}_{k-1/2} + \left(\mathbf{M} - \frac{1}{2}\delta t\,\mathbf{K}\right) \cdot \mathbf{u}_{k-1}, \; k \ge 1,$$

From [21, Th.1.6] we have the following convergence result.

Theorem 2.4. *Let the assumptions of Theorem 2.2 hold true. Further, let u_k^h, $k \geq 0$, be the solution to (2.7), (2.6), and let there exist $K > 0$ independent of h such that for all $r \in [1, 2]$:*

$$\|u_0^h(x) - u_0(x)\|_{L^2(\Omega)} \leq K\, h^r \|u_0(x)\|_{H^r(\Omega)}$$

and $u_0(x) = 0$ on Γ. Then, there exists $C > 0$ such that for $k \geq 0$ and $r \in [1, 2]$ it holds that

$$\|u_k^h(x) - u(x, t_k)\|_{L^2(\Omega)} \leq C\, h^r \left(\|u_0(x)\|_{H^r(\Omega)} + \int_0^{t_k} \left\| \frac{\partial u}{\partial s}(x, s) \right\|_{H^r(\Omega)} ds \right) +$$

$$C\,(\delta t)^2 \int_0^{t_k} \left(\left\| \frac{\partial^3 u}{\partial s^3}(x, s) \right\|_{L^2(\Omega)} + \left\| \triangle_x \left(\frac{\partial^2 u}{\partial s^2}(x, s) \right) \right\|_{L^2(\Omega)} \right) ds.$$

3. Domain decomposition coupled with parareal

We introduce parallelism into the numerical solution procedures for the FEM semi-discretized system (2.3). We include parallelization in time by means of the parareal method as well as parallelization in space by means of domain decomposition methods for the auxiliary pseudo-stationary linear systems (2.5) or (2.7) arising at each time step.

3.1. **Parareal.** We adopt the following parallel strategy for solution to (2.3). We split the time interval $I = (0, T)$ into M nonoverlapping, for simplicity, equidistant subintervals (T_k, T_{k+1}), $k = 0, 1, \ldots, M - 1$, where $T_k := k\,\Delta T$ and $\Delta T := T/M$, $M \ll m$. Given a solution estimate on the coarse time-grid $\mathbf{U}_k \approx \mathbf{u}(T_k)$ for $k = 0, 1, \ldots, M - 1$, where $\mathbf{U}_0 := \mathbf{u}_0$, we solve the following M smaller problems in parallel:

$$(3.1) \qquad \begin{cases} \mathbf{M} \cdot \mathbf{u}_k'(t) + \mathbf{K} \cdot \mathbf{u}_k(t) &= \mathbf{b}(t) \qquad \forall t \in I_k := (T_k, T_{k+1}), \\ \mathbf{u}_k(T_k) &= \mathbf{U}_k. \end{cases}$$

In this way we predict the solution $\mathbf{u}(t) \approx \mathbf{u}_k(t)$ on I_k up to the error, which is the solution to the following homogeneous system over I:

(3.2)
$$\begin{cases} \mathbf{M} \cdot \mathbf{e}_k'(t) + \mathbf{K} \cdot \mathbf{e}_k(t) &= \mathbf{0} & \forall t \in I_k \ \forall k \in \{0, 1, \ldots, M - 1\}, \\ \mathbf{e}_k(T_k) - \mathbf{e}_{k-1}(T_k) &= \mathbf{u}_{k-1}(T_k) - \mathbf{U}_k & \forall k \in \{1, 2, \ldots, M - 1\}, \\ \mathbf{e}_0(0) &= \mathbf{0}. \end{cases}$$

The idea of the parareal method [14] is to alternate the predictor, which is solution to (3.1) using a fine scheme, typically with time-step δt, and the corrector, which is

solution to (3.2) using a coarse scheme, typically with time-step ΔT. Obviously, after i such predictor-corrector steps we get the true solution $\mathbf{u}(t)$ on $[0, T_i]$. Nevertheless, the parareal method converges super-linearly [11] with respect to ΔT also on the yet unresolved interval $(T_i, T]$. In fact, the parallel speedup, i.e. the number of parallel processes times the ratio between the computational time of the sequential algorithm and the computational time of the parallel one, is roughly inversely proportional to the number of iterations, cf. [4].

We shall summarize the parareal algorithm. Denoting by $\boldsymbol{\mathcal{I}}_{\delta t}(T_k, T_{k+1}, \mathbf{U}_k)$ a one-step numerical solution procedure to (3.1) and assuming the same one-step method for the solution of (3.2), but now with the time-step ΔT, the parareal method can be written in the following condensed form: Given the initial coarse prediction $\mathbf{U}_{k+1}^0 := \boldsymbol{\mathcal{I}}_{\Delta T}(T_k, T_{k+1}, \mathbf{U}_k^0)$ with $\mathbf{U}_0^0 := \mathbf{u}_0$, the i-th iteration of the parareal reads

$$(3.3) \qquad \mathbf{U}_{k+1}^{i+1} = \boldsymbol{\mathcal{I}}_{\Delta T}(T_k, T_{k+1}, \mathbf{U}_k^{i+1}) - \boldsymbol{\mathcal{I}}_{\Delta T}(T_k, T_{k+1}, \mathbf{U}_k^i) + \underbrace{\boldsymbol{\mathcal{I}}_{\delta t}(T_k, T_{k+1}, \mathbf{U}_k^i)}_{=: \mathbf{U}_{k+1}^{i+1/2} \approx \mathbf{u}_k(T_{k+1})}$$

for $k = 0, 1, \ldots, M-1$. The last term on the right-hand side of (3.3) is the fine-grid predictor while the remainder is the coarse-grid corrector, which, e.g., in case of the backward Euler method (2.5) reads as follows:

$$\left(\frac{1}{\Delta T}\mathbf{M} + \mathbf{K}\right) \cdot \underbrace{\left(\mathbf{U}_{k+1}^{i+1} - \mathbf{U}_{k+1}^{i+1/2}\right)}_{\approx \mathbf{e}_k(T_{k+1})}$$

$$- \frac{1}{\Delta T}\mathbf{M} \cdot \underbrace{\left[\underbrace{\left(\mathbf{U}_k^{i+1} - \mathbf{U}_k^{i+1/2}\right)}_{\approx \mathbf{e}_{k-1}(T_k)} + \underbrace{\left(\mathbf{U}_k^{i+1/2} - \mathbf{U}_k^i\right)}_{\approx \mathbf{u}_{k-1}(T_k) - \mathbf{U}_k}\right]}_{\approx \mathbf{e}_k(T_k)} = \mathbf{0}, \quad k = 0, 1, \ldots, M-1,$$

where $\mathbf{U}_0^i = \mathbf{u}_0$. Hence, (3.3) indeed coincides with (3.1) and (3.2).

3.2. **Domain Decomposition Methods.** Assuming a one-step time integrator, at each time step of the temporal fine-grid predictor (3.1) as well as the coarse-grid corrector (3.2) a linear system, e.g. (2.5) or (2.7), is solved. Since it is an FEM discretization of an elliptic problem we can employ a spatial DDM to increase the parallelism. We opt for a Schur complement method [1, 15] in the 2-dimensional case. Since in the 1-dimensional counterpart the Schur complement method is simply the direct solve, we employ an overlapping Schwarz method to justify the robustness of the parareal.

3.2.1. *2-dimensional Schur complement DDM.* Let us denote the symmetric and positive-definite system arising at an iteration of the one-step time integration scheme of (2.3) by

$$(3.4) \qquad\qquad \mathbf{A} \cdot \mathbf{u} = \mathbf{b}.$$

We shall describe the domain decomposition method referring to Fig. 1. We follow the presentation in [15]. We assume that besides the FEM triangulation the computational domain $\Omega \subset \mathbb{R}^2$ is decomposed into N nonoverlapping triangular or rectangular subdomains Ω_i, $i = 1, \ldots, N$, of a typical diameter H so that the interface, the so-called skeleton, aligns with the finite element triangulation of a typical diameter h, $h \ll H$. We group the FEM basis functions $\phi_1, \ldots, \phi_n \in V_h$ into $N + 1$ sets as follows:

- In the first set I_1 we take indices whose basis functions have supports in $\overline{\Omega_1}$,
- in the second set I_2 we collect indices whose basis functions have supports in $\overline{\Omega_2}$,
- ...
- In the set I_N we pick indices whose basis functions have supports in $\overline{\Omega_N}$.
- Finally, we take the remaining indices I_S whose basis functions are associated to the nodes along the skeleton or the Neumann part Γ_N of the boundary.
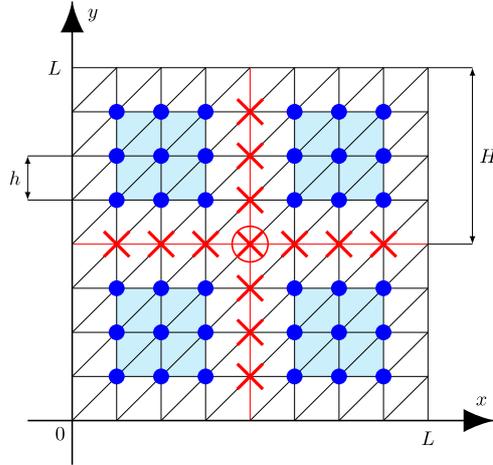

FIGURE 1. Discretization of the spatial domain.

After this perturbation of indices the upper-left block of the system (3.4) becomes block-diagonal, which we exploit in the following solution procedure, the first and last step of which can be performed by N concurrent processes:

(1) $\mathbf{A}_{I_i,I_i} \cdot \mathbf{u}_{I_i}^{\mathrm{P}} = \mathbf{b}_{I_i}$ for $i = 1, 2, \ldots, N$,

(2) $\mathbf{S} \cdot \mathbf{u}_{I_S}^{\mathrm{H}} = \mathbf{b}_{I_S} - \sum_{i=1}^{N} \mathbf{A}_{I_S,I_i} \cdot \mathbf{u}_{I_i}^{\mathrm{P}}$,

(3) $\mathbf{A}_{I_i,I_i} \cdot \mathbf{u}_{I_i}^{\mathrm{H}} = -\mathbf{A}_{I_i,I_S} \cdot \mathbf{u}_{I_S}^{\mathrm{H}}$ for $i = 1, 2, \ldots, N$,

where $\mathbf{S} := \mathbf{A}_{I_S,I_S} - \sum_{i=1}^{N} \mathbf{A}_{I_S,I_i} \cdot (\mathbf{A}_{I_i,I_i})^{-1} \cdot \mathbf{A}_{I_i,I_S}$. The solution (up to the permutation) is $\mathbf{u} = \mathbf{u}^{\mathrm{H}} + \mathbf{u}^{\mathrm{P}}$.

The idea of the DDM of our choice, the so-called vertex-based method [1, 22, 15], is to replace the costly Schur complement $\mathbf{S}$ by an approximation $\widehat{\mathbf{S}}$. We rely on the observation that $\mathbf{S}$ is a blockwise sparse matrix with the sparsity pattern corresponding to the graph of the skeleton. Namely, only the pairs of basis functions that are associated to a common subdomain Ω_i have a nonzero contribution in $\mathbf{S}$. To exploit this property we number all the edges, including those along Γ_{N}, of the skeleton $1, 2, \ldots, N_E$ and group the skeleton indices I_S into the following subsets:

- In the first set I_1^E we take indices adjacent to the interior nodes of the first edge,
- ...
- In the set $I_{N_E}^E$ we pick indices adjacent to the interior nodes of the last edge.
- In the set I^V we collect the remaining nodes, which are called vertices. Either they are shared by at least three subdomains, or they are end-points of a Neumann edge.

We abbreviate the union of all the edge sets by I^E. We denote the number of elements in a set I by $|I|$. Furthermore, referring to Fig. 2, we replace the vertex basis functions, the support of which covers only the adjacent finite element triangles, with basis functions of the support enlarged to the adjacent subdomains. Note that since
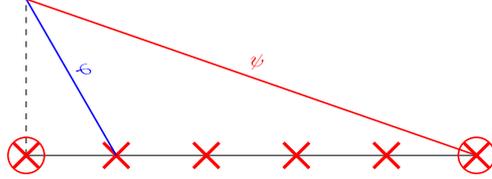

FIGURE 2. Extension of a basis function.

we consider only triangular or rectangular subdomains, the latter transformation of vertex basis functions is linear and the FEM coordinates of the transformed vertex basis functions are columns of $\begin{pmatrix} \mathbf{R}^E \\ \mathbf{I}^V \end{pmatrix}$, where $\mathbf{I}^V \in \mathbb{R}^{|I^V| \times |I^V|}$ is the identity matrix and $\mathbf{R}^E \in \mathbb{R}^{|I^E| \times |I^V|}$ realizes the linear interpolation of the new vertex functions onto the interior nodes along the adjacent edges. Denoting by $\mathbf{I}^E \in \mathbb{R}^{|I^E| \times |I^E|}$ the

identity matrix, the Schur complement is represented as follows:

$$\mathbf{S} = \begin{pmatrix} \mathbf{I}^E & \mathbf{0} \\ -\mathbf{R}^E & \mathbf{I}^V \end{pmatrix} \cdot \begin{pmatrix} \mathbf{S}_{I^E,I^E} & \widetilde{\mathbf{S}}_{I^E,I^V} \\ \widetilde{\mathbf{S}}_{I^V,I^E} & \widetilde{\mathbf{S}}_{I^V,I^V} \end{pmatrix} \cdot \begin{pmatrix} \mathbf{I}^E & -(\mathbf{R}^E)^T \\ \mathbf{0} & \mathbf{I}^V \end{pmatrix}.$$

In this representation the matrix $\widetilde{\mathbf{S}}_{I^V,I^V}$ is nothing but the FEM discretization of the same bilinear form using the new vertex functions. This is why we shall denote it by $\mathbf{A}^H := \widetilde{\mathbf{S}}_{I^V,I^V}$. It gives rise to a spatial coarse-grid solver.

Finally, in the Schur complement approximation $\widehat{\mathbf{S}}$ we neglect the off-diagonal matrices $\widetilde{\mathbf{S}}_{I^V,I^E}$, $\widetilde{\mathbf{S}}_{I^E,I^V}$, and we also replace the edge-edge interaction matrix $\mathbf{S}_{I^E,I^E}$ by its block-diagonal part $\widehat{\mathbf{S}}_{I^E,I^E} := \mathrm{diag}\left(\mathbf{S}_{I_1^E,I_1^E}, \ldots, \mathbf{S}_{I_{N_E}^E,I_{N_E}^E}\right)$. We arrive at the following representation of the approximate Schur complement inverse:

$$\widehat{\mathbf{S}}^{-1} = \sum_{i=1}^{N_E} \left(\mathbf{R}_{I_i^E,*}^E\right)^T \cdot \left(\mathbf{S}_{I_i^E,I_i^E}\right)^{-1} \cdot \mathbf{R}_{I_i^E,*}^E + \left(\begin{pmatrix} \mathbf{R}^E \\ \mathbf{I}^V \end{pmatrix}^T\right) \cdot \left(\mathbf{A}^H\right)^{-1} \cdot \begin{pmatrix} \mathbf{R}^E & \mathbf{I}^V \end{pmatrix}.$$

The action of this matrix to a vector comprises solution to N_E independent Dirichlet problems formulated on pairs of subdomains that are adjacent to a common skeleton edge. Further, the action of $\widehat{\mathbf{S}}^{-1}$ involves solution to a coarse-grid problem arising from the same operator, which is now discretized by the FEM on the DDM skeleton grid. It is proven [15] that the condition number of this preconditioned system is

$$\kappa\left(\widehat{\mathbf{S}}^{-1} \cdot \mathbf{S}\right) \leq C \left(1 + \log \frac{H}{h}\right)^2,$$

where C depends only on the shape of Ω, provided quasi-uniformity and shape-regularity of both the DDM decomposition and the FEM discretization and assuming that eventual jumps of bilinear form coefficients align with the DDM discretization.

3.2.2. *1-dimensional overlapping Schwarz DDM.* We decompose the spatial interval $\Omega := (0, L)$ into N equidistant subintervals to which we add an overlap $\delta \in (0, H)$, $H := L/N$, i.e., $\Omega_k := (\min\{(k-1)H - \delta, 0\}, \max\{kH + \delta, L\})$. The overlapping Schwarz DDM applied to a boundary value problem for an elliptic PDE, e.g., the following Dirichlet problem:

$$\begin{cases} -\mathrm{div}\left(k(x)\nabla u(x)\right) + m(x)\,u(x) &= f(x), \quad x \in \Omega, \\ u(0) = u(L) &= 0, \end{cases}$$

is an iterative procedure, where in the iterations $i = 1, 2, \ldots$ the following $k = 1, 2, \ldots, N$ Dirichlet auxiliary subproblems are solved in parallel:

$$(3.5) \quad \begin{cases} -\mathrm{div}\left(k(x)\nabla u_k^i(x)\right) + m(x)\,u_k^i(x) &= f(x), & x \in \Omega_k, \\ u_k^i(kH - \delta) &= u_{k-1}^{i-1}(kH - \delta), & k > 1, \\ u_k^i(kH + \delta) &= u_{k+1}^{i-1}(kH + \delta), & k < N, \\ u_1^i(0) = u_N^i(L) &= 0. \end{cases}$$

The problems (3.5) are discretized by the FEM with a step-size $h \ll H$.

4. Numerical experiments

We present three kinds of numerical results. In Section 4.1 we confirm the theoretically predicted convergence rates of the finite element semi-discretization combined with the two time-stepping schemes. In Section 4.2 we show robustness of the convergence of the parareal method with respect to the number of temporal subdomains. Finally, in Section 4.3 we display robustness of the combinations of the parareal with the Schur complement DDM in 2 dimensions as well as with the overlapping Schwarz method in 1 spatial dimension. In all these studies we shall consider problem (2.1) with the following setup:

$$(4.1) \quad c(x) := 25, \ k(x) := 1, \ f(x,t) := 0, \ \Omega := (0,1)^d, \Gamma_D := \Gamma, \ \Gamma_N := \emptyset, \ T := 2,$$

$$u_0(x) := \prod_{i=1}^{d} \sin(\pi x_i),$$

where $d \in \{1,2\}$ is the spatial dimension.

4.1. Convergence of discretized solutions.
We present convergence rates of the approximate solutions (2.6) using the backward Euler (2.5) and the Crank-Nicolson (2.7) time-stepping schemes in 1 spatial dimension at the final time $t := T$. The 1-dimensional, $d := 1$, exact solution to (2.1) with setup (4.1) is as follows:

$$u(x,t) := \sin(\pi x) \, e^{-\frac{\pi^2}{c} t}.$$

We study error of $u^{h,\delta t}(x,T) := u_m^h(x)$, which is the discretized solution (2.6) at time $T = m \, \delta t$. The spatial and temporal steps are equal, $h = \delta t$. As predicted by Theorems 2.3 and 2.4, respectively, in Tab. 1 we observe the linear convergence of the backward Euler scheme and the quadratic convergence of the Crank-Nicolson scheme in the L^2-norm. In Tab. 2 we show that the convergence in the H^1-seminorm is only

$h = \delta t$	1/4	1/8	1/16	1/32	1/64
backward Euler	1.81e−2	2.22e−3	1.34e−3	1.10e−3	6.65e−4
Crank-Nicolson	2.96e−2	7.60e−3	1.91e−3	4.79e−4	1.20e−4

TABLE 1. Convergence in the L^2-norm $\|u(x,T) - u^{h,\delta t}(x,T)\|_{L^2(\Omega)}$.

linear in both cases. The quadratic convergence for the Crank-Nicolson scheme would require a higher-order finite element approximation in space.

$h = \delta t$	1/4	1/8	1/16	1/32	1/64
backward Euler	2.26e−1	1.14e−1	5.76e−2	2.89e−2	1.45e−2
Crank-Nicolson	2.30e−1	1.15e−1	5.72e−2	2.86e−2	1.43e−2

TABLE 2. Convergence in the H^1-seminorm $|u(x,T) - u^{h,\delta t}(x,T)|_{H^1(\Omega)}$.

4.2. **Robustness of parareal.** We fix the spatial and temporal discretization steps, $h := 1/32$ and $\delta t := 1/512$, respectively, and we choose the backward Euler scheme. We shall study the following L^2-error of the parareal iterations,

$$
(4.2) \qquad \frac{\left\| u_{\mathrm{parareal}}^{h,\delta t,\Delta T,i}(x,T) - u^{h,\delta t}(x,T) \right\|_{L^2(\Omega)}}{\left\| u^{h,\delta t}(x,T) \right\|_{L^2(\Omega)}},
$$

where

$$
u_{\mathrm{parareal}}^{h,\delta t,\Delta T,i}(x,T) := \sum_{j=1}^{n} (\mathbf{U}_M^i)_j \, \phi_j(x),
$$

which is the approximation (3.3) of the i-th iteration of the parareal method at the time $T = M \, \Delta T$. In Tab. 3 we can see that in order to achieve a given precision (e.g., 1e−8) the number of iterations decreases ($i = 6, 5, 5$) with an increasing parallelism in time ($\Delta T = 1/4, 1/8, 1/16$). This means that the overall complexity of the predictor steps enjoys optimal parallel scalability. In practice the parallel speedup is partly deteoriated by the sequential corrector steps.

ΔT	$i := 1$	$i := 2$	$i := 3$	$i := 4$	$i := 5$	$i := 6$
1/2	2.04e−1	1.28e−2	2.62e−4	0	0	0
1/4	1.28e−1	6.72e−3	1.93e−4	3.33e−6	3.86e−8	1.87e−9
1/8	7.08e−2	2.28e−3	4.52e−5	6.20e−7	8.10e−9	1.29e−9
1/16	3.70e−2	6.53e−4	7.41e−6	6.09e−8	5.18e−10	5.78e−11

TABLE 3. Relative error (4.2) of parareal iterations for the 2d problem.

4.3. **Robustness of DDM coupled with parareal.** Finally, we present numerical results of the novel combination of the parareal method coupled with the Schur complement DDM in 2 spatial dimensions. Again, we fix the spatial and temporal discretization steps, $h := 1/32$ and $\delta t := 1/512$, respectively, and we choose the backward Euler scheme. We shall study error (4.2) of the parareal iterations, but now the arising linear systems (2.5) are solved by the preconditioned conjugate gradients (PCG) method up to the relative precision 1e−8 using the Schur complement DDM preconditioner of Section 3.2.1. The results in Tab. 4 show the error after three

parareal iterations. We observe that the convergence in the column $i := 3$ of Tab. 3 is not affected. Moreover, the convergence is independent of the spatial parallelism and it is again improving with the increasing parallelism in time. Note that the maximal numbers of PCG iterations were 6, 15, 27, and 21, respectively, for the DDM parameters $H := 1/2, 1/4, 1/8$, and $1/16$.

ΔT	$H := 1/2$	$H := 1/4$	$H := 1/8$	$H := 1/16$
1/2	2.62e−4	2.62e−4	2.62e−4	2.62e−4
1/4	1.92e−4	1.92e−4	1.92e−4	1.92e−4
1/8	4.40e−5	4.40e−5	4.40e−5	4.40e−5
1/16	6.95e−6	6.95e−6	6.96e−6	6.95e−6

TABLE 4. Relative error (4.2) after 3 parareal-DDM iterations in 2d.

In Tab. 5 we present results of a 1 dimensional counterpart to the previous table. Here we fix the discretization steps to $h := 1/256$ and $\delta t := 1/512$ and we choose the backward Euler scheme. We combine the parareal method with the 1-dimensional overlapping Schwarz DDM of Section 3.2.2, where we fix the overlap to $\delta := H/4$ and we fix the number of PCG iterations for the solution to systems (2.5) to 7. The results are depicted in Tab. 5. As usual we observe acceleration of the convergence when increasing the parallelism in time. On the other hand, the convergence deteoriates with increasing parallelism in space, since there is no coarse problem in the alternating Schwarz method that we use.

ΔT	$H := 1/2$	$H := 1/4$	$H := 1/8$	$H := 1/16$	$H := 1/32$
1/16	1.32e−9	1.32e−9	3.98e−8	8.79e−4	1.59e0
1/32	5.83e−11	5.87e−11	4.69e−11	9.70e−5	2.08e−1
1/64	2.55e−12	2.85e−12	3.55e−12	9.82e−7	1.54e−2
1/128	3.28e−13	5.94e−13	1.22e−12	1.81e−8	1.10e−3
1/256	2.34e−13	4.78e−13	1.05e−12	8.82e−10	1.21e−4

TABLE 5. Relative error (4.2) after 3 parareal-DDM iterations in 1d.

5. CONCLUSION

In this paper we dealt with a combination of the parareal and domain decomposition methods for the transient heat equation in 1 and 2 spatial dimensions. We recalled the convergence theory of the FEM semi-discretization and two time-stepping schemes and we confirmed the theory by numerical experiments in 1d. Further, we recalled the parareal method, the 2d vertex-based Schur complement DDM and the 1d overlapping Schwarz DDM and we presented novel combinations of the parareal

and DDM with numerical results indicating robustness of the new method. This paper is intended as an initial study. Yet, massively parallel simulations are needed, which will be together with space-time Galerkin approach presented in a near future.

References

[1] *J.H. Bramble, J.E. Pasciak, A.H. Schatz*: The construction of preconditioners for elliptic problems by substructuring, I. Math. Comput. **47** (1986), 103–134.

[2] *X. Dai, Y. Maday*: Stable parareal in time method for first- and second-order hyperbolic systems. SIAM J. Sci. Comput. **35** (2013), A52–A78.

[3] *R.D. Falgout, T.V. Kolev, S.P. MacLachlan, J.B. Schroder*: Parallel time integration with multigrid. SIAM J. Sci. Comput. **36** (2014), C635–C661.

[4] *C. Farhat, M. Chandesris*: Time-decomposed parallel time-integrators: thory and feasibility studies for fluid, structure, and fluid—structure applications. Internat. J. Numer. Methods Engrg. **58** (2003), 1397–1434.

[5] *C. Farhat, F.-X. Roux*: A method of finite element tearing and interconnecting and its parallel solution algorithm. Internat. J. Numer. Methods Engrg. **32** (1991), 1205–1227.

[6] *M.J. Gander*: 50 years of time parallel time integration. In T. Carraro, M. Geiger, S. Körkel, R. Rannacher (eds.) Multiple Shooting and Time Domain Decomposition Methods, pp. 69–113, Springer, 2015.

[7] *M.J. Gander, L. Halpern, F. Nataf*: Optimal Schwarz waveform relaxation for the one dimensional wave equation. SIAM J. Numer. Anal. **41** (2003), 1643–1681.

[8] *M.J. Gander, Y-L. Jiang, R-J. Li*: Parareal Schwarz waveform relaxation methods. In: R. Bank, M. Holst, O. Widlund, J. Xu (eds) Domain Decomposition Methods in Science and Engineering XX, pp. 451–458, Springer, 2013.

[9] *M.J. Gander, F. Kwok, B.C. Mandal*: Dirichlet-Neumann and Neumann-Neumann waveform relaxation algorithms for parabolic problems. Electron. Trans. Numer. Anal. **45** (2016), 424–456.

[10] *M.J. Gander, M. Neumüller*: Analysis of a new space-time parallel multigrid algorithm for parabolic problems. SIAM J. Sci. Comput. **38** (2016), A2173–A2208.

[11] *M.J. Gander, S. Vandewalle*: Analysis of the parareal time-parallel time-integration method. SIAM J. Sci. Comput. **29** (2007), 556–578.

[12] *M.J. Gander, S. Vandewalle*: On the superlinear and linear convergence of the parareal algorithm. In: O.B. Widlund, D.E. Keyes D.E. (eds.) Domain Decomposition Methods in Science and Engineering XVI, pp. 291–298, Springer, 2007.

[13] *L. He*: The reduced basis technique as a coarse solver for parareal in time simulations. J. Comput. Math. **28** (2010), 676–692.

[14] *J.-L. Lions, Y. Maday, G. Turinici*: Résolution d'EDP par un schéma en temps 'pararéel'. C. R. Acad. Sci. Paris, Série I, **332** (2001), 661–668.

[15] *D. Lukáš, J. Bouchala, P. Vodstrčil, L. Malý*: 2-Dimensional Primal Domain Decomposition Theory in Detail. Appl. Math. **60** (2015), 265–283.

[16] *J. Mandel, M. Brezina*: Balancing domain decomposition for problems with large jumps in coefficients. Math. Comp. **65** (1996), 1387–1401.

[17] *D. Mercerat, L. Guillot, J-P. Vilotte*: Application of the parareal algorithm for acoustic wave propagation. AIP Conf. Proc. 1168 (2009), 1521–1524.

[18] *M. Neumüller*: Space-Time Methods: Fast Solvers and Applications. Monographic Series TU Graz, 2013.

[19] *S. Schöps, I. Niyonzima, M. Clemens*: Parallel-in-time simulation of eddy current problems using parareal. IEEE Trans. Magn. **54** (2018), 7200604.

[20] *B.F. Smith, P.E. Bjørstad, W.D. Gropp*: Domain Decomposition — Parallel Multilevel Methods for Elliptic Partial Differential Equations, Cambridge University Press, 1996.

[21] *V. Thomée*: Galerkin Finite Element Methods for Parabolic Problems, Springer, 2006.

[22] *A. Toselli, O. Widlund*: Domain Decomposition Methods — Algorithms and Theory, Springer, 2005.

[23] *E. Zeidler*: Nonlinear Functional Analysis and its Applications II/A — Linear Monotone Operators, Springer, 1990.

Authors' addresses: *Ladislav Foltyn*, Department of Applied Mathematics, Faculty of Electrical Engineering and Computer Science & IT4Innovations, VŠB–Technical University of Ostrava, 17. listopadu 15, 708 00 Ostrava-Poruba, Czech Republic; *Dalibor Lukáš* (corresponding author), Department of Applied Mathematics, Faculty of Electrical Engineering and Computer Science, VŠB–Technical University of Ostrava, 17. listopadu 15, 708 00 Ostrava-Poruba, Czech Republic, e-mail: `dalibor.lukas@vsb.cz`; *Ivo Peterek*, Department of Applied Mathematics, Faculty of Electrical Engineering and Computer Science & IT4Innovations, VŠB–Technical University of Ostrava, 17. listopadu 15, 708 00 Ostrava-Poruba, Czech Republic.